

Curie temperature, exchange integrals, and magneto-optical properties in off-stoichiometric bismuth iron garnet epitaxial films

B. Vertruyen,^{1,*} R. Cloots,¹ J. S. Abell,² T. J. Jackson,² R. C. da Silva,³ E. Popova,⁴ and N. Keller⁴

¹*SUPRATECS/LCIS, Chemistry Institute B6, University of Liege, B-4000 Liege, Belgium*

²*School of Engineering, The University of Birmingham, B15 2TT Edgbaston, Birmingham, United Kingdom*

³*Laboratório de Feixes de Iões, Departamento Física, Instituto Tecnológico e Nuclear, Sacavém, Portugal*

⁴*Groupe d'Etude de la Matière Condensée (GEMaC), CNRS-UVSQ, 45 Avenue des Etats-Unis, 78035 Versailles Cedex, France*

(Received 22 November 2007; revised manuscript received 25 June 2008; published 30 September 2008)

We have studied the influence of the stoichiometry on the structural, magnetic, and magneto-optical properties of bismuth iron garnet ($\text{Bi}_3\text{Fe}_5\text{O}_{12}$) thin films grown by pulsed laser deposition. Films with different stoichiometries have been obtained by varying the Bi/Fe ratio of the target and the oxygen pressure during deposition. Stoichiometry variations influence the Curie temperature T_C by tuning the (Fe)-O-[Fe] geometry: T_C increases when the lattice parameter decreases, contrary to what happens in the case of stoichiometric rare-earth iron garnets. The thermal variation of the magnetization, the Faraday rotation, and the Faraday ellipticity have been analyzed in the frame of the Néel two-sublattice magnetization model giving energies of -48 K (4.1 meV), -29 K (2.5 meV), and 84 K (7.3 meV) for the three magnetic exchange integrals j_{aa} , j_{dd} , and j_{ad} , respectively. Magneto-optical spectroscopy linked to compositional analysis by Rutherford backscattering spectroscopy shows that Bi and/or Fe deficiencies also affect the spectral variation (between 1.77 and 3.1 eV). Our results suggest that bismuth deficiency has an effect on the magneto-optical response of the tetrahedral Fe sublattice, whereas small iron deficiencies affect predominantly the magneto-optical response of the octahedral sublattice.

DOI: [10.1103/PhysRevB.78.094429](https://doi.org/10.1103/PhysRevB.78.094429)

PACS number(s): 75.50.Gg, 78.20.Ls, 75.30.Et, 61.50.Nw

I. INTRODUCTION

Bismuth substitution on the dodecahedral site of ferrimagnetic iron garnets is known to enhance drastically the Faraday rotation in visible light (Ref. 1 and references therein). Apart from the obvious interest of these Bi-substituted compounds in view of applications,²⁻⁹ there has also been much attention paid to the theoretical aspects (see Ref. 10) especially concerning the influence of Bi on the spectral dependence of the magneto-optical properties.¹¹⁻¹⁹ However, studies on the role of bismuth in iron garnets have long been confined to compounds with relatively low bismuth content because the pure bismuth iron garnet $\text{Bi}_3\text{Fe}_5\text{O}_{12}$ (BIG) does not exist in bulk form (due to the large ionic radius of the Bi^{3+} cation) and cannot be grown by liquid-phase epitaxy (LPE). Since 1989, several authors have shown that BIG can be grown as a thin film on suitable garnet substrates by pulsed laser deposition (PLD),^{4,6,18,20-28} reactive ion-beam sputtering (RIBS) (Refs. 29-31), or other vapor deposition techniques.³²⁻³⁴ Much information has been gained through these works but comparison of the available data for BIG films reveals a significant dispersion of the experimental results. For example, Curie temperatures vary between 618 and 643 K (Refs. 21, 31, 35, and 36) and typical values of the saturation magnetization $\mu_0 M_s$ range from 0.12 to 0.165 T.^{20,22-24,30,31} The cubic lattice parameter is certainly an influential parameter since, depending on the garnet substrate, the film lattice-parameter values vary between 1.2619 and 1.2671 nm.^{22,23,28,30-33,37} However, another important issue is the stoichiometry of the films: contrary to liquid phase epitaxy, vapor phase deposition techniques, such as used to grow BIG films frequently yield off-stoichiometric films,³⁸ and the reported Bi/Fe ratios vary indeed in a wide range (from 0.48 to 0.66).^{22,26,28,30,33,34,39}

In the present paper we study the effect of variations to the stoichiometry of bismuth iron garnet thin films on the magnetic and magneto-optical properties. We report on the temperature dependence (100–700 K) of the Faraday rotation and ellipticity at a photon energy of 2.25 eV for BIG films grown by PLD under different oxygen pressures and from targets of different compositions. These magneto-optical properties give us access to the magnetization and the Curie temperature. The magnetic sublattice exchange integrals are obtained by a self-consistent calculation and fitting of the Néel two-sublattice model to the experimental data. The relations of the Curie temperature and exchange integrals with the lattice parameter and the stoichiometry of the films are discussed in Sec. III B.

These parameters also appear to affect the spectral dependence (1.77 to 3.1 eV) of the Faraday rotation and ellipticity at room temperature. In the literature, the quantitative analysis of the influence of bismuth substitution on the Faraday rotation spectra has attracted much interest¹¹⁻¹⁹ but was mainly investigated on stoichiometric films grown by LPE, i.e., with relatively low bismuth content. Building on ideas from Dionne and Allen,^{11,12} Helseth *et al.*^{13,14} analyzed the Faraday rotation spectra with a simple model based on two optical transitions. Recently, Dionne and Allen¹⁵ have discussed the concept of intersublattice transitions and proposed a crystalline electric level scheme based on molecular-orbital hybrid states. This analysis allowed them to assign the observed transition energies in the experimental dielectric functions to excitations occurring on the tetrahedral and octahedral sites of Fe-O polyhedra. Another approach proposed by Zenkov and Moskvina^{16,17} based on a semiquantitative model calculating explicitly the charge-transfer transitions in the octahedral (FeO_6)⁹⁻ and tetrahedral (FeO_4)⁵⁻ complexes

TABLE I. Nominal Bi/Fe ratio in target, $P(\text{O}_2)$ during deposition and cooling, film thickness measured by RBS, Bi/Fe ratio in film, Bi deficiency $\{\delta_{\text{Bi}}=(3-x_{\text{Bi}})/3\}$, and Fe deficiency $\{\delta_{\text{Fe}}=(5-x_{\text{Fe}})/5\}$ measured by RBS, crystallographic cell parameter a , Curie temperature T_C , room-temperature saturation magnetization $\mu_0 M_s$, and coercive field $\mu_0 H_C$

Film	Bi/Fe target	P_{O_2} (mTorr)	d (nm)	Bi/Fe (RBS)	δ_{Bi} (RBS)	δ_{Fe} (RBS)	a (nm)	T_C (K)	$\mu_0 M_s$ (T)	$\mu_0 H_C$ (mT)
A	3/5	500	805	0.50	0.20	0.03	1.2621 ± 0.0005	701	0.113 ± 0.024	6.5
B	3/5	250	430	0.49	0.25	0.08	1.2616 ± 0.0005	695	0.127 ± 0.018	6.9
C	3/5	50	690	0.50	0.20	0.03	1.2638 ± 0.0005	687	0.133 ± 0.023	7.3
D	3.15/5	50	400	≤ 0.59	≥ 0.06	0.04	1.2639 ± 0.0005	675	0.142 ± 0.020	4.5
E	3.3/5	50	400	0.61	0.04	0.05	1.2653 ± 0.0005	653	0.140 ± 0.019	3.6

gives a quantitative basis to the semiempirical assignment of the observed transition energies to excitations occurring in different Fe-O coordinations. Concerning the description of the electronic structure, these two approaches used to be the only means to assign the observed transitions to excitations in the Fe-O polyhedra. Only very recently, the first fully relativistic band-structure calculation performed by Oikawa *et al.*¹⁹ reporting a density-functional theory calculation of the electronic structure of $\text{Bi}_3\text{Fe}_5\text{O}_{12}$ became available. Concerning completely substituted (and possibly nonstoichiometric) $\text{Bi}_3\text{Fe}_5\text{O}_{12}$, studies giving an interpretation of the observed optical and magneto-optical transition lines within the frame of the above sketched theoretical interpretations are scarce: Kahl *et al.*¹⁸ found that a single diamagnetic transition seems to be sufficient to describe the Faraday rotation spectrum between 1.24 and 2.4 eV. In Sec. III C, we use the simple two-transition model based on the works by Zenkov *et al.*,^{16,17} Dionne *et al.*,^{11,12,15} and Helseth *et al.*^{13,14} to suggest a qualitative link between the modified spectral response and a possible site preference for the cationic vacancies.

II. EXPERIMENTAL METHODS

BIG films were deposited on $5 \times 5 \text{ mm}^2$ (001) $\text{Gd}_3\text{Ga}_5\text{O}_{12}$ (GGG) substrates by laser ablation with a KrF excimer laser (Lambda Physik LPX210, $\lambda=248 \text{ nm}$, pulse energy density $\sim 2.5 \text{ J/cm}^2$, and a repetition rate of 50 Hz). Targets with different compositions were used. The first was a commercial target with 3/5 nominal Bi/Fe ratio. The other two were prepared by standard solid state reaction of Bi_2O_3 and $\text{FeC}_2\text{O}_4 \cdot 2\text{H}_2\text{O}$ with nominal Bi/Fe ratios of 3.15/5 and 3.3/5. The distance between the substrate and the target was 5.5 cm. The temperature of the substrate holder was kept at 570 °C during deposition. The films were cooled at 10 °C/min immediately after ablation. The deposition parameters for each film can be found in Table I.

General x-ray diffraction characterization was performed with a four-circle Siemens D5000 diffractometer (Cu K_α radiation). Cu $K_{\alpha 1}$ $\theta/2\theta$ scans and rocking curves were collected with a PANalytical X'Pert PRO MRD for precise determination of the cell parameters.

The composition of the films was studied by Rutherford backscattering spectroscopy (RBS). The films were irradiated with 2 MeV $^4\text{He}^+$ ions with beam currents of 1–3 nA and total accumulated charges of 1–2 μC . All spectra were

normalized to 1 μC charge. The RBS spectra were collected with two semiconductor Si detectors, placed at angles of 140° and slightly less than 180° with respect to the incoming beam direction, and having energy resolutions of 13 and 16 keV, respectively. For each film, two sets of spectra were taken sequentially in the same conditions in order to make sure that the analyzing beam did not induce any change in the samples due to ion irradiation. In all cases the spectra overlapped entirely. The spectra were obtained under 3° tilt in order to avoid channeling.

Temperature-dependent Faraday rotation measurements have been performed using a custom-designed magneto-optical magnetometer.⁴⁰ The samples were mounted successively in a high-temperature furnace and in a liquid nitrogen cryostat allowing variation of the sample temperature from 100 to 900 K. Measurements were performed at fixed photon energies of 1.77, 1.90, 2.06, 2.25, 2.48, 2.76, 3.10 eV and in spectroscopic mode with a second setup based on a phase modulation technique using a commercial charge coupled device (CCD) spectrometer.

III. RESULTS AND DISCUSSION

A. Structure and composition of the films

The homogeneity and epitaxy of all films were characterized by x-ray diffraction. Each $\theta/2\theta$ pattern displays the (00 l) peaks of the GGG substrate and the BIG garnet film as shown in Fig. 1 for film C. This confirms that the garnet phase is obtained for a rather large range of experimental conditions as reported by most other authors.^{26,30} Tepper *et al.*²⁸ reported a narrower window of deposition conditions, maybe due to the fact that they used a low laser energy density for the deposition (1.4 J/cm^2). Traces of BiFeO_3 are observed in films A, C, and E. Slightly more intense BiFeO_3 peaks are found in film D. Adachi *et al.*²² also detected a weak BiFeO_3 peak in films grown by PLD with oxygen pressure above 30 mTorr. Epitaxial cube-on-cube growth is confirmed by Φ scans of the (4010) reflection (see inset of Fig. 1). The typical full width at half maximum (FWHM) of the (008) BIG reflection is in the range 0.20°–0.25° similar to other published work for growth on GGG substrates.^{24,32} By using substrates with a better lattice match, such as GSGG,²² the FWHM can be reduced to 0.06°. The lattice parameters determined for our films are reported in Table I. They were obtained by applying the Nelson-Riley extrapolation.^{22,41}

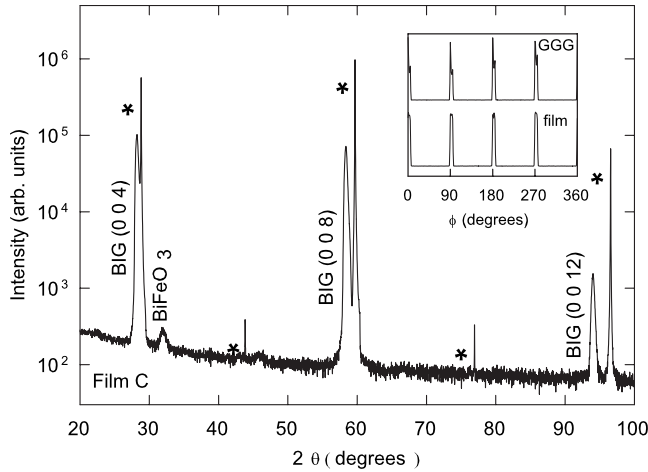


FIG. 1. X-ray diffraction results. Main figure: $K_{\alpha 1}$ $\theta/2\theta$ scan of film C in logarithmic scale. GGG reflections are marked by an asterisk. Inset: Φ scan of the (4010) reflection.

Lattice parameters published for BIG in the literature vary between 1.2620 and 1.2671 nm with an average value of $a = 1.2632 \pm 0.0015$ nm.^{22,23,28,30–33,37} More specifically, for BIG growth on GGG substrate, the observed lattice parameters vary in the range of 1.2619 to 1.2635 nm.^{28,32} In the present work, the lattice parameters vary between 1.2616 and 1.2653 nm depending on the oxygen pressure and target composition.

The composition of the films was studied by RBS. RBS channeling experiments were performed in order to discard the influence of channeling on the experimental data and confirmed the rather good epitaxial quality of the films. For film C, the channeling quality (given by the ratio of RBS yields in aligned and off-aligned situations) is about 22% (to be compared to less than 4% for the single-crystalline GGG substrate). Figure 2 shows the RBS experimental data and the simulated spectrum in the case of film E. It was not possible to reproduce the fine details of the RBS spectra with a constant composition description. For all films, the results suggest an overall decrease of the Bi/Fe ratio from the BIG/GGG interface to the BIG surface as also observed

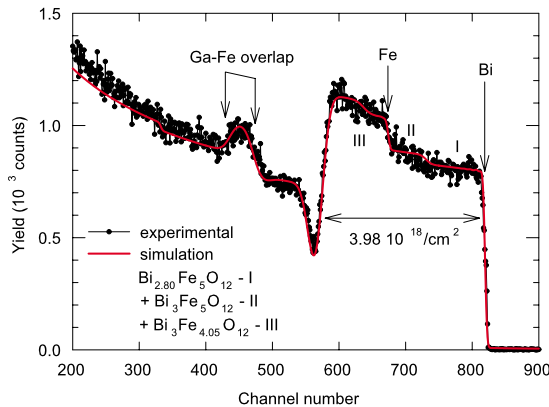


FIG. 2. (Color online) RBS spectrum of film E. The experimental data are fitted by a model with three layers of decreasing Bi/Fe ratio from the BIG/GGG interface to the BIG surface.

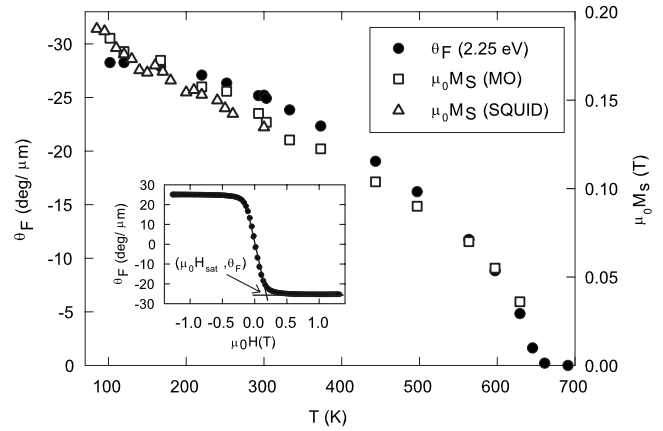


FIG. 3. Temperature dependence of the Faraday rotation measured at $E=2.25$ eV, of the saturation magnetization, and of the saturation magnetization measured by SQUID for film E. The inset shows a typical hysteresis loop $\theta_F(H)$ indicating how the values of Faraday rotation and magnetization are determined. H_{sat} is the saturation field (see text for details).

by other authors for BIG films deposited by PLD.^{28,39} Previously, Krumme *et al.*⁴² had concluded from their experiments on Bi-substituted iron garnet films grown by rf magnetron sputtering that the Bi-O bond is weaker than other metal-oxygen bonds in iron garnets. The average values for Bi/Fe ratio, Bi deficiency $\{\delta_{\text{Bi}}=(3-x_{\text{Bi}})/3\}$, and Fe deficiency $\{\delta_{\text{Fe}}=(5-x_{\text{Fe}})/5\}$ can be found in Table I. Since some BiFeO₃ was detected by x-ray diffraction, the Bi/Fe ratio in the garnet phase could be somewhat overestimated especially for film D. These RBS stoichiometry data suggest that films deposited from the stoichiometric target (films A, B, and C) are strongly Bi-deficient as also observed by other authors.^{26,39} Films D and E were grown from targets containing a bismuth excess and have a Bi/Fe ratio close to the nominal value of 0.6.

The variations of crystallographic parameter and composition will be discussed later in this paper in relation with the magneto(-optical) properties.

B. Temperature dependence of the magnetization and the Faraday rotation

The temperature dependence of the saturation magnetization M_S can be determined using magneto-optical Faraday rotation measurements.³⁸ Using the anisotropy constants reported by Adachi *et al.*²² for BIG films, it can be shown that the magnetocrystalline anisotropy field H_K is approximately one order of magnitude smaller than the demagnetizing field H_d (with $H_d \approx M_S$ when H is perpendicular to the film plane). Therefore, the extrapolated magnetic saturation field $\{\mu_0 H_{\text{sat}} = \mu_0 (H_d + H_K)\}$ indicated by the arrow in the inset of Fig. 3 can be used to determine the saturation magnetization M_S when neglecting H_K in the first approximation. The room-temperature magnetization values are given in Table I. A maximum value of $\mu_0 M_S \approx 0.14$ T is obtained for the stoichiometric BIG films (films D and E). Typical values reported in the literature are in the range 0.12–0.165 T for films grown by PLD or RIBS on various substrates.^{20,22–24,30,31}

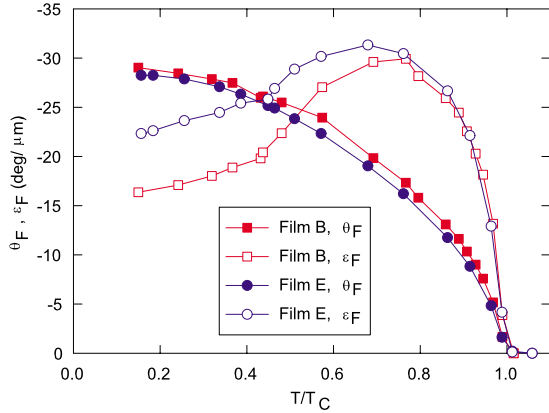


FIG. 4. (Color online) Temperature dependence of the Faraday rotation (θ_F) and ellipticity (ϵ_F) at $E=2.25$ eV as a function of reduced temperature T/T_C for films *B* and *E*. Plain lines are guides for the eye.

Films *D* and *E* display the lowest coercive fields of the series (~ 4 mT), which is two and four times smaller than the coercive fields determined by Kahl *et al.*²⁴ and Okuda *et al.*,³³ respectively.

Figure 3 shows the typical temperature dependence of the Faraday rotation (full dots) as measured on film *E* for a photon energy of 2.25 eV and in the temperature range of 100 to 700 K. The same figure compares the saturation magnetization values deduced from the Faraday rotation data as described above (square symbols) with the values measured with a superconducting quantum interference device (SQUID) magnetometer (open triangles). The SQUID data agree well with the magnetization data obtained from the Faraday hysteresis loops confirming that H_K is small compared to M_S . The temperature dependence of the Faraday rotation of BIG displays a regular decrease of θ_F with increasing temperature, contrary to the case of yttrium iron garnet (YIG),^{38,43–46} for which the presence of two magnetic sublattices is evidenced by a maximum at ~ 350 K. This trend on Bi substitution had already been observed by Hansen *et al.*⁴⁴ for $Y_{3-x}Bi_xFe_5O_{12}$ ($x \leq 1.44$) compounds. Although the temperature dependence of the Faraday rotation of BIG might look as if only one magnetic sublattice were present, the normalized temperature dependence (T/T_C) of the ellipticity displayed in Fig. 4 clearly confirms the presence of the two magnetic sublattices (tetrahedral and octahedral Fe-O polyhedra) via a pronounced maximum. As in the case of YIG (see Ref. 38), the observed maximum here in the Faraday ellipticity does shift with changes to stoichiometry and could be an indicator of the relative occupation of octahedral and tetrahedral iron sites. The magneto-optical spectroscopy data discussed in Sec. III C seem to indicate that film *B* presents an increased iron deficiency of the octahedral Fe-O polyhedron leading to an increase in the reduced temperature of the maximum in Faraday ellipticity as has been observed for $\theta_F(T)$ in YIG.³⁸

Another important property of a magnetic material is the Curie temperature as it is directly related to the exchange integrals. All determined Curie temperatures can be found in Table I. These values ranging between 653 and 701 K are

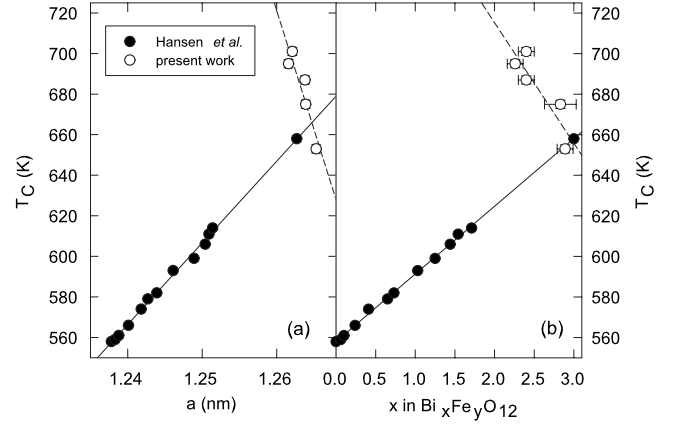


FIG. 5. Curie temperature as a function of (a) cubic cell parameter and (b) Bi content in the film. Black symbols are data taken from Hansen *et al.* (Refs. 44–46) for (Y,Bi)IG films. The point at 1.263 nm; $x_{Bi}=3$ results from a linear extrapolation of these data. Empty symbols are the data from the present work. The dashed line is a linear fit to these data.

higher than the experimental values reported in the literature,^{21,31,35,36} which do not exceed 643 K.³¹ The Curie temperatures for the Bi-deficient films are even higher than the value of 672 K extrapolated from the data of Hansen *et al.*⁴⁵ for Bi-substituted YIG. Figures 5(a) and 5(b) give a graphical representation of the measured Curie temperatures as a function of the lattice parameter [Fig. 5(a)] and of the bismuth content [Fig. 5(b)] compared with data taken from literature (solid circles) on bismuth substituted YIG films grown by LPE.^{44–46} It can be seen that nonstoichiometry affects strongly the Curie temperature. Compared to Bi-substituted YIG films,⁴⁴ Bi-deficient BIG films display inverse dependencies of T_C on lattice parameter a and bismuth concentration x_{Bi} , i.e., T_C tends to increase when a or x_{Bi} decreases.

1. Analysis of magnetization data

The thermal variation of the magnetization, the Faraday rotation, and the Faraday ellipticity can be described in the frame of Néel model as the result of two antiferromagnetic (AF) coupled sublattices. Formally, the magnetization of $Bi_3Fe_5O_{12}$ is given by (cf. Ref 47)

$$M(T) = M_d(T) - M_a(T), \quad (1)$$

where M_d and M_a are the magnetization of the tetrahedral and octahedral sublattices, respectively.

Each sublattice magnetization is given by

$$M_i(T) = M_i(0)B_{si}(x_i), \quad (2)$$

where $B_{si}(x_i)$ represents the Brillouin function of the i th sublattice ($i=a, d$),

$$B_{si} = \frac{2S_i + 1}{2S_i} \coth \left[\left(\frac{2S_i + 1}{2S_i} \right) x_i \right] - \frac{1}{2S_i} \coth \left[\left(\frac{1}{2S_i} \right) x_i \right], \quad (3)$$

and

$$M_d(0) = 3gS_d\mu_B N_A f_d, \quad M_a(0) = 3gS_a\mu_B N_A f_a. \quad (4)$$

Here the constants f_a and f_d have been introduced to allow for a variation of the zero-temperature magnetization in each sublattice. S_k represents the spin quantum numbers of the magnetic ions with $S_k=5/2$ for Fe^{3+} in the high spin state. μ_B is the Bohr magneton ($=9.2741 \times 10^{-24}$ J/T), k_B is the Boltzmann constant ($=1.3807 \times 10^{-23}$ J/K), and N_A is the Avogadro constant ($=6.022 \times 10^{23}$ mol $^{-1}$).

The coefficients x_d and x_a are given by

$$x_d = \frac{S_d g \mu_B}{k_B T} (N_{dd} M_d + N_{da} M_a), \quad x_a = \frac{S_a g \mu_B}{k_B T} (N_{aa} M_a + N_{ad} M_d) \quad (5)$$

and $N_{ik} = (2Z_{ik} J_{ik}) / (n_k g_i g_k \mu_B^2)$, where Z_{ik} is the number of nearest neighbors, n_k is the number of ions per mole in the k th sublattice, J_{ik} is the exchange integral ($J_{ad} = J_{da}$), and g_i is the spectroscopic splitting factor of each sublattice ($=2.0$). Equation (1) can be self-consistently solved in order to obtain the exchange integrals J_{ik} , which govern the magnetic order and which determine the Curie temperature of the system. In order to perform suitable numerical adjustment of Eq. (1) to the experimental data, it is preferable to normalize Eqs. (1)–(5) in order to express them in units of μ_B . The magnetization scales as $n_B = M_S / \mu_B N_A$. Normalizing Eqs. (1)–(5), one obtains for the reduced magnetization,

$$n_B(T) = 3gS_d f_d B_{sd}(x_d^*) - 2gS_a f_a B_{sa}(x_a^*) \quad (6)$$

with

$$x_d^* = \frac{2S_d}{gT} (j_{dd} n_d + j_{da} n_a), \quad x_a^* = \frac{2S_a}{gT} (j_{aa} n_a + j_{ad} n_d), \quad (7)$$

$$j_{kl} = J_{kl} / k_B,$$

where j_{kl} is expressed in kelvins. Now the magneto-optical Faraday rotation and ellipticity are both proportional to a combination of the individual sublattice magnetizations weighted by a proportionality factor. One may write them as follows:

$$\theta_F(T) = C_{V,d} 3gS_d f_d B_{sd}(x_d^*) - C_{V,a} 2gS_a f_a B_{sa}(x_a^*),$$

$$\varepsilon_F(T) = C_{E,d} 3gS_d f_d B_{sd}(x_d^*) - C_{E,a} 2gS_a f_a B_{sa}(x_a^*). \quad (8)$$

Equations (6) and (8) were integrated into a nonlinear least-mean-square fitting algorithm using a self-consistent determination of each sublattice magnetization for the adjustable parameters (j_{ik} , f_i , $C_{v,i}$, and $C_{e,i}$ with $i=a,d$). The algorithm allows for a simultaneous adjustment of Eqs. (6) and (8) to the respective data sets. The obtained fitting for film A is given in Fig. 6 where the magnetization, the Faraday rotation, and the Faraday ellipticity have been adjusted. The figure shows the calculated thermal variations for M_S , θ_F , and ε_F and the two sublattice magnetizations of the tetrahedral and octahedral sublattice (dashed lines). Figure 7 gives the results of this analysis for the exchange integrals j_{aa} , j_{dd} , and j_{ad} as a function of the lattice parameter [Fig. 7(a)] and as a function of both the bismuth deficit, δ_{Bi} [Fig. 7(b)], and the iron deficit, δ_{Fe} [Fig. 7(c)]. The experimentally determined

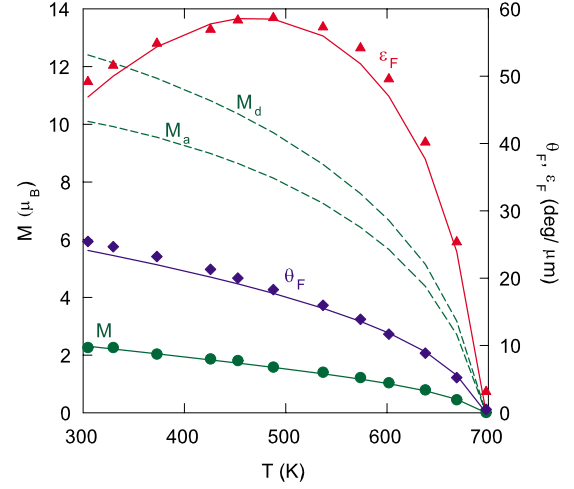


FIG. 6. (Color online) Temperature dependence of the magnetization (circles), Faraday rotation (diamonds) and ellipticity (triangles) for film A shown with the corresponding numerical fits (plain lines; see text for details), and with the calculated sublattice magnetization for the octahedral (M_a) and tetrahedral (M_d) sublattices (dashed lines).

Curie temperatures are also displayed on the same figures. Both j_{aa} and j_{dd} have negative values characteristic of ferromagnetic interactions, whereas j_{ad} is positive revealing the expected antiferromagnetic intersublattice coupling. For our BIG films, typical values of -48 K (4.1 meV), -29 K (2.5 meV), and 84 K (7.3 meV) are obtained for j_{aa} , j_{dd} , and j_{ad} , respectively. The corresponding energies for YIG are -65 K (5.6 meV), -30 K (2.6 meV), and 97 K (8.4 meV).⁴⁷ Globally, the relative values for BIG are in the same order of magnitude compared to YIG. In BIG films, increasing the lattice parameter [Fig. 7(a)] appears to weaken the j_{ad} interaction and strengthen the j_{aa} and j_{dd} interactions, whereas increasing δ_{Bi} [Fig. 7(b)] strengthens the j_{ad} interaction and weakens the other intersublattice interactions.

The Curie temperature and exchange integrals are strongly influenced by the geometry of the [Fe]-O-(Fe) unit where [Fe] is an iron ion in octahedral site, and (Fe) is an iron ion in tetrahedral site. Therefore, it is interesting to examine the literature data concerning the influence of a cell parameter variation on the local iron-oxygen geometry in iron garnets. Iron garnets are usually indexed in the cubic $Ia-3d$ space group⁴⁸ with iron and rare-earth ions on fixed special positions. Therefore, the [Fe]-O-(Fe) angle is uniquely determined by the fractional coordinates of the oxygen ion, while the [Fe]-O and (Fe)-O distances can be expressed as a function of the cell parameter and the oxygen coordinates. As a result, an increase of the cell parameter is linked to variations of the [Fe]-O-(Fe) angle and/or [Fe]-O and (Fe)-O distances. Crystallographic data with refined oxygen parameters are required to discuss this issue. Data for $R_3\text{Fe}_5\text{O}_{12}$ ($R=\text{Yb, Tm, Er, Ho, Dy, Y, Tb, Gd, and Eu}$) can be found in the powder diffraction file (PDF)-4 crystallographic database⁴⁹ and in Ref. 50. The increase of T_C when the rare-earth radius and the cell parameter increase⁴⁸ seems to be linked to a small increase of the [Fe]-O-(Fe) angle without significant variation of the [Fe]-O and (Fe)-O distances.

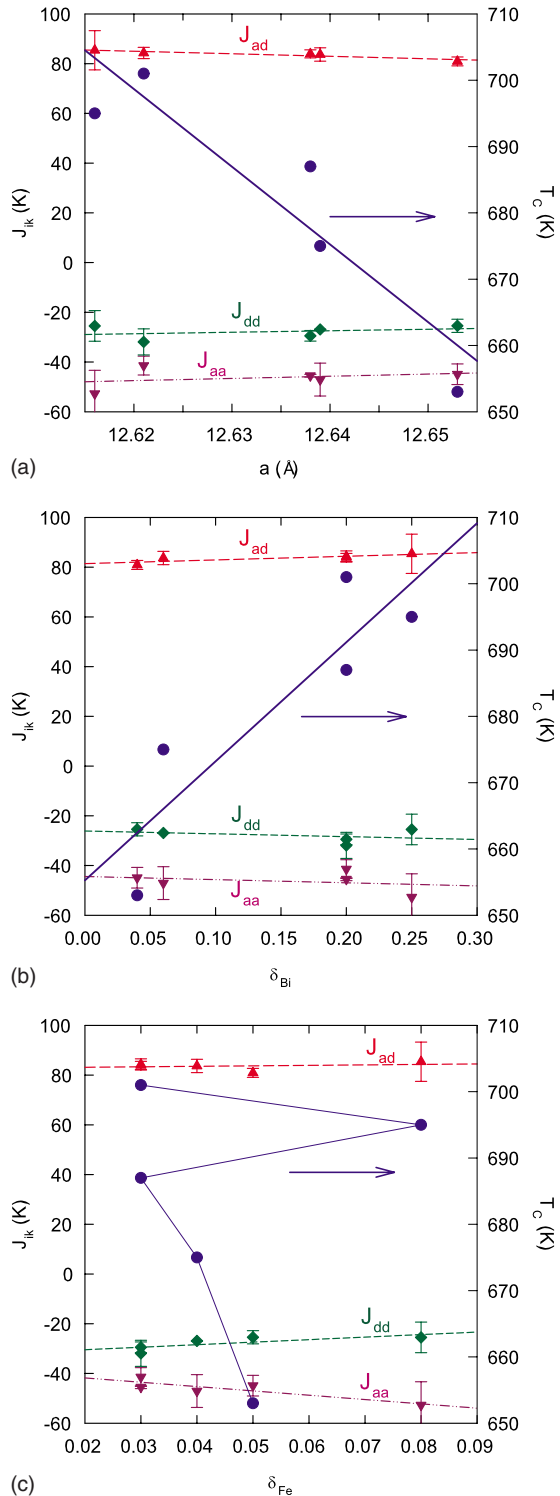


FIG. 7. (Color online) The numerically determined exchange integrals (j_{aa} , j_{dd} , and j_{ad}) and the corresponding experimental Curie temperature of the BIG films as a function of (a) the lattice parameter, (b) the bismuth deficit δ_{Bi} , and (c) the iron deficit δ_{Fe} .

However, these variations are too small [e.g., [Fe]-O-(Fe) angle varies between 125° and 127°] to draw firm conclusions. Indeed Geller and Colville⁵¹ reached opposite conclusions when characterizing an $Y_{1.12}Bi_{1.88}Fe_5O_{12}$ single crystal. They observed that the increase in cell parameter (due to

bismuth substitution in YIG) seems to be linked to a decrease in the (Fe)-O distance and an increase in the [Fe]-O distance without significant variation of the sum of the [Fe]-O and (Fe)-O distances and without variation of the [Fe]-O-(Fe) angle. But these variations are very small and the cationic mixture on the dodecahedral site implies that only average values are obtained. Therefore, it would be highly interesting to have reliable crystallographic data on $Bi_3Fe_5O_{12}$, but this is made difficult by the fact that this compound exists only as a film. Toraya *et al.*³⁷ have attempted a Rietveld refinement of x-ray diffraction data of a polycrystalline BIG film deposited on a garnet buffer layer. With respect to YIG, they found a large decrease in the (Fe)-O distance and a large increase in the [Fe]-O distance without significant variation of the [Fe]-O-(Fe) angle. However, the (Fe)-O distance (~ 1.79 Å) seems unrealistically small for a (Fe³⁺)-O distance (usually ~ 1.87 Å), and the O-(Fe)-O angles suggest an unusually large distortion of the FeO_4 tetrahedron. On the other hand, a geometry optimization of the oxygen position in BIG has recently been calculated by Oikawa *et al.*¹⁹ and predicts an increase of the [Fe]-O-(Fe) angle of $\sim 4^\circ$ without significant variation of the [Fe]-O and (Fe)-O distances when BIG is compared to YIG. The same authors¹⁹ obtained similar results when they calculated the oxygen coordinates using the empirical relation established by Hawthorne⁵² through multiple-regression analysis of structural data taken from more than 40 garnet compositions. It is of interest to note that the O-(Fe)-O and O-[Fe]-O angles predicted by Oikawa *et al.*¹⁹ correspond to significantly smaller distortions of the octahedra and tetrahedra than in the $R_3Fe_5O_{12}$ compounds discussed above ($R=Yb-Eu$).^{49,50}

The above discussion suggests that an increase in the [Fe]-O-(Fe) angle might be involved in the T_c increase observed in stoichiometric iron garnets when the cell parameter increases. This interpretation is consistent with the angular variation of the superexchange integral in ferrimagnetic iron garnets.⁵³ However, our discussion only takes into account geometrical effects and considers cation- and oxygen-stoichiometric compounds. The results in Fig. 5 for the series of BIG films clearly show that nonstoichiometry (both in oxygen and metal ion content) affects strongly the Curie temperature. While “stoichiometric” BIG films *D* and *E* reasonably agree with the linear extrapolations derived from results for Bi-substituted YIG,⁴⁴ Bi-deficient BIG films display inverse dependencies of T_c on lattice parameter a and bismuth concentration x_{Bi} , i.e., T_c tends to *increase* when a or x_{Bi} *decreases*.

Indeed cationic or oxygen vacancies are expected to modify effectively the [Fe]-O-(Fe) geometrical environment and superexchange integral. Considering the large number of parameters involved (angles, distances, spin-orbit coupling, iron oxidation state, etc.), it is difficult to identify the physical mechanism without theoretical simulations of nonstoichiometric garnet models. Considering the analysis of the magnetization data (see above), the observed trends for j_{ad} , j_{aa} , and j_{dd} suggest that in off-stoichiometric BIG, a decrease in the lattice parameter or an increasing bismuth deficit results in changes in the local [Fe]-O-(Fe) geometry such that the antiferromagnetic exchange between octahedral and tetrahedral iron ions is favored, thereby, enhancing the Curie temperature.

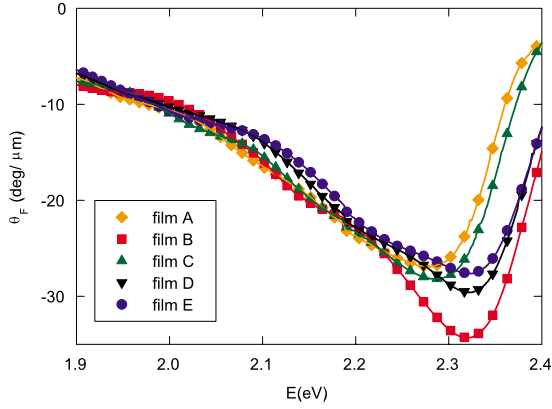


FIG. 8. (Color online) Room-temperature spectral variation of the Faraday rotation peak centered around ~ 2.3 eV.

It is worth pointing out that the highest T_C is observed for film A characterized by comparatively large Bi deficiency, small cell parameter, and small magnetization. Since this film was grown in an oxygen-rich atmosphere and is probably not oxygen-deficient, electroneutrality suggests that Fe^{4+} ions might be present. This would be consistent with the small cell parameter because Fe^{4+} is smaller than Fe^{3+} .^{54,55} Also because of its size, Fe^{4+} is expected to be located on the tetrahedral site, which is consistent with the small value of saturation magnetization. A small (Fe)-O distance would enhance the overlap integral and thereby the exchange integral and Curie temperature. This interpretation is consistent with a previous hydrostatic pressure study of YIG.⁵⁶ In this study, it has been demonstrated that the Curie temperature of YIG increases linearly with increasing hydrostatic pressure. When linked to the variation of T_C with decreasing lattice parameter, one can obtain a quantitative estimate of the change to T_C for BIG. For YIG, a variation of T_C with changes in lattice parameter, $T_C = -1.25 \times 10^4 \times \Delta a$, has been determined by Podsekin *et al.*⁵⁷ Using the experimentally observed decrease in the lattice parameter for BIG of $\Delta a \approx 0.002$ nm (Table I), an increase of $\Delta T_C \approx 25$ K is obtained. This increase perfectly accounts for the experimentally observed increase in T_C (see Table I).

C. Room-temperature magneto-optical properties

The Faraday rotation (θ_F) and ellipticity (ϵ_F) of the films were measured as functions of magnetic field at different photon energies. A value of $-25^\circ/\mu\text{m}$ for the specific Faraday rotation was observed at a photon energy of 2.25 eV confirming literature results.^{25,29,33} The largest specific Faraday rotation ($\sim 34^\circ/\mu\text{m}$) was observed for an energy of 2.76 eV. The measured spectral variation agrees well with the results of Chern *et al.*²¹ for $\text{Y}_{3-x}\text{Bi}_x\text{Fe}_5\text{O}_{12}$ ($0.5 \leq x \leq 3.0$) films deposited by PLD.

A second magneto-optical setup based on a rotating compensator method was used to measure the spectral variation of the principal Faraday rotation peak (centered at ~ 2.3 eV). Figure 8 shows the specific Faraday rotation for all films in the spectral range of 1.9 to 2.4 eV. Films B, D, and E exhibit the same spectral variation with a pronounced

peak at ~ 2.32 eV, whereas this peak occurs at lower energies of ~ 2.27 eV for films A and C. It must be pointed out that films A and C are somewhat thicker than films B, D, and E. A qualitatively similar red shift was observed by Kahl *et al.*^{25,26} when increasing the thickness of BIG films grown in otherwise identical conditions. These authors could not identify the cause of this apparent thickness dependence of the red shift, although a possible correlation with the x-ray coherence length was detected by x-ray diffraction. Besides, in the present case, the observed shift is somewhat larger (by $\sim 35\%$) than predicted by the equation extrapolated by Kahl *et al.*²⁶ $\{\Delta E(\text{eV}) \sim -7.93 \times 10^{-5} (\text{eV}/\text{nm}) \times \Delta d(\text{nm})\}$. We discuss now these observations in relation to the different target compositions and oxygen pressures used for the film growth. We have seen above that variations of these experimental parameters result in variations of the stoichiometry, the lattice parameter, and the physical properties, such as the Curie temperature and the three exchange integrals j_{aa} , j_{dd} , and j_{ad} . Such changes should also result in modifications of the spectroscopic magneto-optical response of the different films. The compositional RBS analysis (see Table I) shows that both films D and E possess a Bi/Fe ratio of 0.6, whereas the other three films (A, B, C) have Bi/Fe ratio of ~ 0.5 . Film B is a particular case because it displays a spectral variation identical to that observed in the “stoichiometric” films D and E while presenting a significant deviation from the ideal Bi/Fe ratio. A more detailed analysis reveals that this film not only shows an enhanced deficiency in Bi content but also an enhanced deficiency in Fe content. In the literature, the spectral variation of the magneto-optical Faraday rotation and ellipticity (or more precisely the off-diagonal permittivity tensor elements) in Bi-substituted iron garnets has been subject to intensive analysis both in terms of molecular-orbital analysis^{10–13,15,18,19} and charge-transfer transitions.^{11,14,16,17,19} These descriptions are based on the identification of the underlying electronic transitions either by a first-principles approach^{16,19} or in terms of phenomenological diamagnetic or paramagnetic transition lines.^{10–13,15,18} Following the frequency dispersion analysis presented by Helseth *et al.*¹³ and applied by Kahl *et al.*,¹⁸ it turns out that within the experimentally accessible spectral range of 1.7 to 3.5 eV, only two “diamagnetic transition lines” are relevant.^{13,16,18} According to Zenkov *et al.*,¹⁶ for weakly Bi-substituted YIG the most intense transition lines correspond to a FeO_6 octahedral (2.78 eV) and a FeO_4 tetrahedral (3.4 eV) $\text{O}2p\text{-Fe}^{3+}$ charge-transfer transition. Hence, one can try to link the observed “red shift” of the rotation maximum to changes in the respective oscillator strengths (f) and the densities of absorbing sites (N). In this model one diamagnetic transition line is related to the octahedral Fe-O polyhedron, whereas the second one is related to the tetrahedral Fe-O polyhedron. In this frame, the observed “red shift” of the Faraday rotation maximum due to an increased Bismuth deficit can be identified with a reduction in either N or f of the tetrahedral Fe-O polyhedra. As a consequence and in order to describe the experimental situation coherently, it is necessary to assume that an increased iron deficiency as observed in film B affects essentially the octahedral Fe-O polyhedra by decreasing either N or f and results in a blue shift of the Faraday rotation maximum.

Interestingly, it is possible to use these ideas, especially the link between red shift and Bi deficiency, to suggest a possible explanation for the results of Kahl *et al.*²⁶ as described above. If one accepts the fact that the Bi/Fe ratio in PLD-grown films is larger at the film-substrate interface (as observed by us, Ref. 28, and Ref. 39), it means that increasing the film thickness would tend to increase the Bi deficiency resulting thereby in a red shift. Since Kahl *et al.*²⁶ used the same target composition for all their films, it is logical that the observed red shift in their case is smaller than when we used targets with different stoichiometries.

IV. CONCLUSION

We have studied the influence of the stoichiometry on the structural, magnetic, and magneto-optical properties of bismuth iron garnet (Bi₃Fe₅O₁₂) thin films grown by pulsed laser deposition. Films with different stoichiometries have been obtained by varying the Bi/Fe ratio of the target and the oxygen pressure during deposition. Stoichiometry variations influence the Curie temperature T_C by tuning the (Fe)-O-[Fe] geometry: T_C increases when the lattice parameter decreases, contrary to what happens in the case of stoichiometric rare-

earth iron garnets. The thermal variation of the magnetization, the Faraday rotation, and the Faraday ellipticity have been analyzed in the frame of the Néel two-sublattice magnetization model giving energies of -48 K (4.1 meV), -29 K (2.5 meV), and 84 K (7.3 meV) for the three magnetic exchange integrals j_{aa} , j_{dd} , and j_{ad} , respectively. Magneto-optical spectroscopy linked to compositional analysis by RBS shows that Bi and/or Fe deficiencies also affect the spectral variation (between 1.77 and 3.1 eV). Our results suggest that bismuth deficiency has an effect on the magneto-optical response of the tetrahedral Fe sublattice, whereas small iron deficiencies affect predominantly the magneto-optical response of the octahedral sublattice.

ACKNOWLEDGMENTS

The authors thank M. Bibes (IEF-CNRS, Orsay, France) for the high-resolution XRD experiments. B.V. thanks FNRS, CGRI, the Royal Military Academy, and the University of Liege (Belgium) for financial support. N.K. acknowledges financial support in the frame of the CNRS/CGRI-FNRS cooperation Project No. 18224. T.J.J. and J.S.A. thank the UK Engineering and Physical Sciences Research Council for financial support.

*Corresponding author; b.vertruyen@ulg.ac.be

¹A. K. Zvezdin and V. A. Kotov, *Modern Magneto-optics and Magneto-optical Materials* (Taylor & Francis, London, 1997).
²C. Holthaus, A. Trifonov, H. Dötsch, and J. Schützmann, *NDT & E Int.* **38**, 129 (2005).
³M. Huang and S. Zhang, *J. Mater. Res.* **15**, 1665 (2000).
⁴K. Kawano, R. A. Chakalov, G. Kong, J. S. Abell, S. Kahl, and A. M. Grishin, *Physica C* **372-376**, 696 (2002).
⁵Ph. Vanderbemden, Z. Hong, T. A. Coombs, S. Denis, M. Ausloos, J. Schwartz, I. B. Rutel, N. H. Babu, D. A. Cardwell, and A. M. Campbell, *Phys. Rev. B* **75**, 174515 (2007).
⁶M. Laulajainen, P. Paturi, J. Raittila, H. Huhtinen, A. B. Abrahamson, N. H. Anderson, and R. Laiho, *J. Magn. Magn. Mater.* **279**, 218 (2004).
⁷M. Inoue and T. Fuji, *J. Appl. Phys.* **81**, 5659 (1997).
⁸M. Inoue, K. Arai, T. Fuji, and M. Abe, *J. Appl. Phys.* **85**, 5768 (1999).
⁹S. I. Khartsev and A. M. Grishin, *Appl. Phys. Lett.* **87**, 122504 (2005).
¹⁰J. Yang, Y. Xu, F. Zhang, and M. Guillot, *J. Phys.: Condens. Matter* **18**, 9287 (2006).
¹¹G. F. Dionne and G. A. Allen, *J. Appl. Phys.* **73**, 6127 (1993).
¹²G. F. Dionne and G. A. Allen, *J. Appl. Phys.* **75**, 6372 (1994).
¹³L. E. Helseth, R. W. Hansen, E. I. Il'yashenko, M. Baziljevich, and T. H. Johansen, *Phys. Rev. B* **64**, 174406 (2001).
¹⁴L. E. Helseth, *J. Phys.: Condens. Matter* **15**, 2227 (2003).
¹⁵G. F. Dionne and G. A. Allen, *J. Appl. Phys.* **95**, 7333 (2004).
¹⁶A. V. Zenkov and A. S. Moskvina, *J. Phys.: Condens. Matter* **14**, 6957 (2002).
¹⁷A. V. Zenkov and A. S. Moskvina, *J. Phys.: Condens. Matter* **15**, 2229 (2003).

¹⁸S. Kahl, V. Popov, and A. M. Grishin, *J. Appl. Phys.* **94**, 5688 (2003); **96**, 1767 (2004).
¹⁹T. Oikawa, S. Suzuki, and K. Nakao, *J. Phys. Soc. Jpn.* **74**, 401 (2005).
²⁰M. Y. Chern and J. S. Liaw, *Jpn. J. Appl. Phys., Part 1* **36**, 1049 (1997).
²¹M. Y. Chern, F. Y. Lo, D. R. Liu, K. Yang, and J. S. Liaw, *Jpn. J. Appl. Phys., Part 1* **38**, 6687 (1999).
²²N. Adachi, V. P. Denysenkov, S. I. Khartsev, A. M. Grishin, and T. Okuda, *J. Appl. Phys.* **88**, 2734 (2000).
²³A. Jalali-Roudsar, V. P. Denysenkov, S. I. Khartsev, A. M. Grishin, N. Adachi, and T. Okuda, *IEEE Trans. Magn.* **37**, 2454 (2001).
²⁴S. Kahl, S. I. Khartsev, A. M. Grishin, K. Kawano, G. Kong, R. A. Chakalov, and J. S. Abell, *J. Appl. Phys.* **91**, 9556 (2002).
²⁵S. Kahl and A. M. Grishin, *J. Appl. Phys.* **93**, 6945 (2003).
²⁶S. Kahl and A. M. Grishin, *J. Magn. Magn. Mater.* **278**, 244 (2004).
²⁷B. M. Simion, R. Ramesh, V. G. Keramidis, G. Thomas, E. Marinero, and R. L. Pfeffer, *J. Appl. Phys.* **76**, 6287 (1994).
²⁸T. Pepper and C. A. Ross, *J. Cryst. Growth* **255**, 324 (2003).
²⁹T. Okuda, T. Katayama, T. Oikawa, H. Yamamoto, and N. Koshizuka, in *Recent Advances in Magnetism and Magnetic Materials*, edited by H. L. Huang and P. C. Kuo, (World Scientific, Singapore, 1989).
³⁰T. Okuda, T. Katayama, H. Kobayashi, and N. Kobayashi, *J. Appl. Phys.* **67**, 4944 (1990).
³¹N. Adachi, T. Okuda, V. P. Denysenkov, A. Jalali-Roudsar, and A. M. Grishin, *J. Magn. Magn. Mater.* **242-245**, 775 (2002).
³²P. Johansson, S. I. Khartsev, and A. M. Grishin, *Thin Solid Films* **515**, 477 (2006).

- ³³T. Okuda, T. Katayama, K. Satoh, and H. Yamamoto, *J. Appl. Phys.* **69**, 4580 (1991).
- ³⁴M. Okada, S. Katayama, and K. Tominaga, *J. Appl. Phys.* **69**, 3566 (1991).
- ³⁵A. T. Thavendrarajah, M. Parvadi-Horvath, and P. E. Wigen, *IEEE Trans. Magn.* **25**, 4015 (1989).
- ³⁶S. Mino, M. Matsuoka, A. Tate, A. Shibukawa, and K. Ono, *Jpn. J. Appl. Phys., Part 1* **31**, 1786 (1992).
- ³⁷H. Toraya and T. Okuda, *J. Phys. Chem. Solids* **56**, 1317 (1995).
- ³⁸Y. Dumont, N. Keller, E. Popova, D. S. Schmool, M. Tessier, S. Bhattacharya, B. Stahl, R. M. C. Da Silva, and M. Guyot, *Phys. Rev. B* **76**, 104413 (2007).
- ³⁹R. Lux, A. Heinrich, S. Leitenmeier, T. Körner, M. Herbort, and B. Stritzker, *J. Appl. Phys.* **100**, 113511 (2006).
- ⁴⁰N. Keller, J. Mistrik, S. Visnovsky, D. S. Schmool, Y. Dumont, P. Renaudin, M. Guyot, and R. Krishnan, *Eur. Phys. J. B* **21**, 67 (2001).
- ⁴¹P. A. Tempest, *J. Appl. Crystallogr.* **10**, 238 (1977).
- ⁴²J. P. Krumme, A. F. Otterloo, P. C. Zalm, and J. Pertruzzello, *J. Appl. Phys.* **64**, 3965 (1988).
- ⁴³S. Wittekoek, T. J. A. Popma, J. M. Robertson, and P. F. Bongers, *Phys. Rev. B* **12**, 2777 (1975).
- ⁴⁴P. Hansen, K. Witter, and W. Tolksdorf, *Phys. Rev. B* **27**, 6608 (1983).
- ⁴⁵P. Hansen, K. Witter, and W. Tolksdorf, *J. Appl. Phys.* **55**, 1052 (1984).
- ⁴⁶P. Hansen and J. P. Krumme, *Thin Solid Films* **114**, 69 (1984).
- ⁴⁷G. Dionne, *J. Appl. Phys.* **41**, 4874 (1970).
- ⁴⁸G. Winkler, *Magnetic Garnets* (Vieweg, Braunschweig, 1981).
- ⁴⁹Powder Diffraction File PDF-4 Database, International Centre for Diffraction Data, PDF Card No. 04-009-8391 (YIG), PDF Card No. 04-009-5650 (TbIG), PDF Card No. 04-007-5211 (GdIG), PDF Card No. 04-006-1590 (EuIG).
- ⁵⁰F. Tcheou, F. Huess, and E. F. Bertaut, *Solid State Commun.* **8**, 1745 (1970).
- ⁵¹S. Geller and A. A. Colville, *AIP Conference Proceedings No. 24* (AIP, New York, 1975), p. 372.
- ⁵²F. C. Hawthorne, *J. Solid State Chem.* **37**, 157 (1981).
- ⁵³M. E. Lines, *Phys. Rev. B* **20**, 3729 (1979).
- ⁵⁴R. D. Shannon, *Acta Crystallogr., Sect. A: Cryst. Phys., Diffraction, Theor. Gen. Crystallogr.* **32**, 751 (1976).
- ⁵⁵W. H. de Roode and C. A. P. W. van de Pavert, *J. Appl. Phys.* **55**, 3115 (1984).
- ⁵⁶D. Bloch, *J. Phys. Chem. Solids* **27**, 881 (1966); G. Bocquillon, C. Loriers-Susse, and J. Loriers, *High Temp. - High Press.* **5**, 161 (1973).
- ⁵⁷K. Podsekina and V. N. Zaitsev, *Sov. Phys. Solid State* **23**, 160 (1981).